Application of Orthogonal Frequency Division Multiplexing with Concatenated Codes for Wireless Broadband Communications

What is presented:

- theoretical and simulated bit error rate performances of concatenated coding schemes with orthogonal frequency division multiplexing (OFDM) in multipath fading channels.

- Outer Reed Solomon code is concatenated with different trellis based inner codes in order to achieve a high coding gain. Trellis coded modulation (TCM), turbo code with multilevel mapping (TC), turbo trellis coded modulation (T-TCM) and convolutional codes (CC) are used as inner codes.

- A 512-carrier OFDM system is selected to facilitate the transmission of bit rates up to 155 Mb/s, while the high gain concatenated scheme is used to obtain a remarkable bit error rate performance.

- An interleaver is introduced between RS outer coder and trellis based inner coder to randomize the burst errors from the inner decoder. A channel interleaver is also introduced to combat the correlated fading of the channel.

- Theoretical upper bound of the bit error rate is obtained for comparison. Windowing is used to reduce the high peak-to-average power ratio of the OFDM signal. Bit error rate performance with the windowing is also presented.

I. INTRODUCTION

- In the next few years, increasing attention to wireless broadband services is expected due to the benefits, primarily mobility and installation flexibility. More generally the demand of wide-band multimedia services arising from wireless users has stimulated particular interest in the design of high quality, high speed (10 Mbit/s and up to 155 Mbit/s) wireless networks, which are able to provide access services and capabilities of broad-band fixed networks.

- It is expected that most future broadband networks will be based on asynchronous transfer mode (ATM). ATM transport is an efficient transmission and multiplexing platform for integrating a variety of fixed and wireless services.

- Third and perhaps second generation wireless access will be integrated with ATM based backbone transport and intelligent networks capable of providing many wireless services. This is because ATM can provide flexible bandwidth assignments. A realistic way to convert conventional synchronous transfer mode (STM) based networks in to ATM networks with wireless multimedia handling capabilities is shown in [1].

- Wireless ATM can satisfy the need of delivering bandwidth on demand to portable terminals. A reliable radio link capable of handling data rates of tens of Mb/s is the critical component to meet this goal. Coded orthogonal frequency division multiplexing is promising solution to this.

- The most popular application of OFDM is for digital audio broadcasting (DAB) [3, 4]. Outside broadcast link, asynchronous digital subscriber lines, digital video broadcasting are potential applications [5, 6].

- In 1998, the IEEE 802.11 standardization group decided to select OFDM as the basis for their new 5GHz standard, targeting a range of data rates from 6 up to 54 Mb/s. This new standard is the first to use OFDM in packet-based communications, while all above-mentioned applications are continuous transmission systems.

- Following the IEEE 802.11 decision, high performance LNA (HIPERLAN) type 2 and multimedia mobile access communication (MMAC) also adopted OFDM for their physical layer standards [8].

- There are several studies done in the area of OFDM for wireless broad band applications. A modem, which can transmit high rate ATM cells over an indoor radio channel, was discussed in [9]. A similar study was done in [10] to transmit variable rate ATM cells over high-speed indoor wireless channels (100 to 155 Mb/s). Radio access to an ATM network is considered in [11], in order to make all broadband services available to mobile stations.

- Especially, a time division duplex frame structure is analyzed and described considering different multiple access techniques. The system operates at 2.5GHz and a channel bandwidth of 8 MHz is assumed. The study concentrates on medium access control (MAC), automatic repeat request (ARQ) and a hand-over protocol, but it does not consider the transmission aspects of OFDM.

- Magic wireless ATM network demonstrator (WAND) and the MEDIAN projects demonstrate prototypes wireless ATM networks operating at a raw data rate from 20 Mb/s up to 155 Mb/s. Both projects will expand the services of the fixed B-ISDN using local wireless broadband transmission. OFDM is for the transmission of B-ISDN originated ATM cells with maximum efficiency. It envisages a transparent data flow from the fixed ATM network to the mobile ATM capable multimedia terminal.

- ***Coded OFDM*** is essential for all the applications discussed above. Transmission over a frequency-selective channel implies that some of the subcarriers are strongly attenuated and cause errors even at high average signal power. In this flat fading situation an efficient channel coding leads to a very high coding gain, especially if soft decision decoding is applied.

- Here we are investigating the bit error rate performance of an OFDM system with some of the powerful forward error correcting codes available today. Trellis coded modulation (TCM), turbo coding (TC), turbo trellis coded modulation (T-TCM) and convolutional code (CC) concatenated with Reed Solomon (RS) code are investigated.

- Turbo codes, the newest code in this family of codes has a very high coding gain [12]. Turbo codes result from concatenation of two recursive systematic convolutional codes.

- Combination of turbo codes with TCM gives a bandwidth efficient coding scheme termed as turbo trellis coded modulation (T-TCM) [13, 14]. T-TCM is an extension of binary turbo codes, where recursive systematic convolutional codes are replaced by recursive systematic TCM codes. Application of T-TCM is preferred where high spectral efficiency and good bit error rate performance is expected [15].

II. SYSTEM DESCRIPTION

- In OFDM, a block of N symbols $\{X_n, n = 0,1,..., N-1\}$ is formed with each symbol modulating one of a set of N sub-carriers, $\{f_n, n = 0,1,..., N-1\}$. The N sub-carriers are chosen to be orthogonal, that is $f_n = n\Delta f$, where $\Delta f = 1/NT$ and T the is original symbol period. The resulting signal in the discrete time domain can be expressed as

$$x_k = \sum_{n=0}^{N-1} X_n e^{j2pnk/N} \tag{1}$$

where $k = 0,1,\ldots N-1$, is the time index. A cyclic prefix (called guard interval) is added to the resulting signal in order to avoid the intersymbol interference (ISI), which occurs in multipath channels. At the receiver the guard interval is removed and only the time interval [0, T] is evaluated. The guard interval is usually a periodic extension of the symbol over the interval [-TCP, 0], resulting a symbol of length [-TCP, T].

A. Peak to average power ratio (PAPR)

The main disadvantage of OFDM is the large PAPR, which is defined as

$$PAPR = \frac{\max |x(t)|^2}{E[|x(t)|^2]} \tag{2}$$

where $x(t)$ is the digital to analog converted signal of x_k given in (1) and $E[x]$ is the expected value of x. When N signals are added with the same phase, they produce a peak power which is N times the average power. Therefore maximum theoretical PAPR of an OFDM signal is N. Several schemes have been proposed to reduce this undesirable high PAPR of the OFDM signal [16-19].

The block diagram of the system is shown in Figure 1. Here μ is the modulation index (number of bits per symbol) of the inner encoder. Therefore input to the inner encoder is μ parallel bits.

The ATM cell-mapping scheme described above is valid for the selected encoder structures, which depends on overall code rate and the signal-mapping scheme used. For different encoder structures a suitable mapping scheme can easily be found in a similar manner.

- We have selected the ATM as the transport technique. The outer RS coder receives the unprotected ATM cells at the transmitter. Four ATM cells are mapped to a single block of data for the RS coder input. The total length of the data word is then 212 bytes. The output code word length is then 244 bytes after being coded by RS (244,212) encoder.

- The output from the RS coder is divided into two data blocks. Four trailing bits (zeros) are appended to each block for trellis termination. The inner encoder maps these two blocks of data into 8PSK signal points when TCM and T-TCM inner codes are used and into 16QAM signal points when turbo code and convolutional code are used. Specifications of the inner codes used are given below.

1. Ungerboeck rate 2/3, 8 states TCM code with 8PSK mapping – Viterbi decoding (TCM1). The encoder is shown in Figure 2.

2. Ungerboeck rate 2/3, 16 states TCM code with 8PSK mapping - Viterbi decoding (TCM2). The encoder is shown in Figure 3

3. T-TCM with Ungerboeck rate 2/3 8 states component code with 50% puncturing and 8PSK mapping, - Iterative decoding with max log MAP algorithm (T-TCM). The encoder polynomial of the component TCM codes is given by

$$G_{3\times 4} = \begin{bmatrix} 1 & 0 & 0 & 1 \\ 0 & 0 & 1 & 1 \\ 0 & 1 & 0 & 0 \end{bmatrix} \qquad (3)$$

   In this recursive systematic code a parity check bit is appended to every two information bits and the resulting triple bits are used to select one of 8PSK symbols according to Ungerboeck's rules. There is no uncoded bit in these RSC codes and hence no parallel transitions in T-TCM. T-TCM encode is shown in Figure 4

4. Turbo code with rate ½, 8 states convolutional component codes with 50% puncturing of parity bits and 16QAM mapping - Iterative decoding with max log MAP algorithm (TC). The generator polynomial of the component recursive systematic convolutional encoder is given by

$$G_{2\times 4} = \begin{bmatrix} 1 & 1 & 0 & 1 \\ 1 & 1 & 1 & 1 \end{bmatrix} \quad (4)$$

5. Convolutional code with 16QAM mapping – Viterbi decoding (CC). The industry standard constraint length 7, rate ½ convolutional code is used. The convolutional encoder having generator polynomials $g1=133_8$ and $g2=171_8$.

- This complex baseband signal is then multiplexed in to 512 orthogonal carriers using the inverse fast Fourier transform (IFFT) processor. The block interleaver used between RS coder and inner encoder converts long error bursts of the inner decoder output to short error bursts with length of a few bytes. These short error bursts are then randomly distributed over RS-code words, which can effectively be corrected by the RS decoder. For a channel with correlated fading, a channel interleaver is introduced at the output of the IFFT processor. The mapping of data (ATM cells) into OFDM symbols is shown in Figure 5.

- The choice of a carrier frequency for a radio system usually depends on its bandwidth and the wave propagation characteristics of the selected frequency in the expected environment of operation. For broadband systems, we have to consider both path loss and impulse response of the channel for the selected frequency. 60GHz band is currently under investigation for broadband wireless applications in both indoor and outdoor environments as it is having desirable properties anticipated [20]. Therefore, we have selected 60GHz frequency for the simulations.

- The selection of suitable number of carriers for the OFDM system depends on several parameters. Assuming enough bandwidth (94MHz) can be allocated in the 60GHz frequency band, the suitable number of carriers are selected using the following relationship.

$$(mN)_{\min} = \frac{R_b T_m}{dR_c} \tag{5}$$

where R_b is the data rate, Tm is the maximum delay spread of the channel, δ is the proportion of the guard interval to the OFDM symbol duration, R_s is the code rate and N is number of sub carriers. System specifications are presented in Table 1.

Table 1 System specifications

Bit rate	155.52Mb/s
Number of carriers	512
Delay spread of the channel	250ns
Number of paths	6
Length of the guard interval	50 (10% of the total OFDM symbol duration)
Speed (for correlated fading)	120km/s
Spectral efficiency	2bits/s/Hz for all schemes
Reed Solomon code	RS(244,212)
Frequency	60GHz
Size of the interleaver between RS code and inner code	10.9μs (4*244 byte interleaver)
Size of the channel interleaver	21.8μs (1024*8 symbol interleaver)
Total interleaver delay	65.4μs

III. FREQUENCY SELECTIVE FADING CHANNEL MODEL

- The discrete channel impulse response of the multipath channel [21] can be expressed as

$$h(t) = \sum_{m=0}^{M-1} h_m e^{j f_m} d(t - t_m) \tag{6}$$

where, M is the number of paths, t_m is the delay corresponding to the m^{th} path, h_m is Rayleigh distributed fading amplitude and f_m is uniformly distributed phase. *It is assumed that the*

channel is static during an OFDM symbol. Then the frequency response of the channel [22] can be found as

$$H_n = \sum_{m=0}^{M-1} \left(h_m e^{jj_m} \right) \; e^{-j2pnm/N}, \; n = 0,1,...,N\text{-}1 \tag{7}$$

where N is the number of sub-carriers of the OFDM scheme. The average signal power and the total multipath power can be normalized to one.

- The frequency response of the channel is thus obtained by taking the FFT of the fading coefficients (as h_m=0 for m>L). Statistical properties of AWGN is same in both time and frequency domains. Therefore, received signal at the output of the FFT processor [22] is obtained by

$$R_n = H_n X_n + Z_n \tag{8}$$

- X_n is the modulated data symbol Z_n is the additive white Gaussian noise. In this case the noise variance depends on the signal to noise ratio (E_b/N_0), code rate (R_c) and the spectral efficiency (η) of the modulation scheme.
- This is given by

$$s_n^2 = \frac{1}{2hR_c(E_b / N_o)} \tag{9}$$

Figure 6 shows the equivalent channel model.

IV. CODING SCHEMES AND DECODING ALGORITHMS

A. Trellis coded modulation (TCM)

- TCM schemes employ redundant non-binary modulation in combination with finite-state encoder, which governs the selection of modulation signals to generate coded signals [23]. In the receiver, a soft-decision maximum likelihood sequence decoder decodes the noisy signals. Non systematic, eight-state encoder depicted in Figure 2 is used in the simulations. Zero bits are appended to both data streams d_0 and d_1 for the trellis termination purpose. The set partition of 8PSK constellation, which achieves higher euclidean distances, is shown in Figure 7 [24]. Corresponding trellis diagram and the signal constellation is depicted in Figure 8.

- Viterbi decoding is done at the receiver. The branch metric of the Viterbi decoder for the OFDM in multipath fading channel is the squared euclidean distance between the received signal and the branch symbol multiplied by the fading coefficient. We have assumed that the perfect channel state information is available at the receiver. The branch matrix (B_n^j) corresponds to the received symbol at the branch can be expressed as

$$B_n^j = \left| R_n - H_n s_n^j \right|^2 \tag{10}$$

Here H_n is given in (6) and s_n^j is the branch symbol (8PSK) corresponds to the j^{th} branch. Both TCM schemes use the above decoding algorithm.

B. Binary turbo code (TC)

- Turbo code is constructed by concatenating two recursive systematic convolutional (RSC) component codes through an interleaver. A random interleaver is used for the simulation. We used a ½ rate 8-state RSCs as component codes, having a generator polynomials given by (3). The code words of the above turbo code consist of the input bits (systematic) followed by the parity check bits from the two encoders. Parity check bits of each RSC output are punctured

alternatively increasing the code rate to ½. The states of trellises are forced to the zero state at the end of each block of information. This process is termed as trellis termination.

C. Turbo trellis coded modulation (T-TCM)

- T-TCM encoder is similar to the turbo encoder structure. But in T-TCM encoder RSCs are replaced by recursive systematic TCM encoders. In this case, the output from the RSC TCM encoders is 8PSK symbols. Random interleaver is again used but this time pair wise interleaving is done. Puncturing the every other symbol from the two encoders alternatively forms output symbol sequence.

- SISO decoder using max log MAP algorithm is used for T-TCM decoding [14]. The logarithm of the transition probability corresponding to the transition from state σ_n to state σ_{n-1} of the trellis can be found as

$$\log[\gamma(s_n, s_{n-1})] = -\log(2\pi\sigma_n^2) - \frac{\left|R_n - H_n s_n^j\right|^2}{2\sigma_n^2} + \log(P_a) \tag{11}$$

$$P_a = p(s_n / s_{n-1}) \tag{12}$$

where R_n is the received symbol, P_a is the a priori information, s_n^j is the branch symbol corresponds to the branch connecting states σ_n to σ_{n-1} and H_n is given by (6). The rest of the decoding process is done as described in [14].

D. Extracting soft values for convolutional code and turbo code decoding

- The 16QAM constellation with Gray mapping is used in both turbo code and convolutional code. The a posteriori probability of transmitted symbol at interval *n* can be expressed as

$$p(s_n^j \mid R_n) = \frac{p(R_n \mid s_n^j)\, p(s_n^j)}{p(r_n)} \tag{13}$$

where s_n^j is the symbols of 16QAM constellation corresponding to the j[th] branch to the trellis. $p(R_n / s_n^j)$ is the conditional probability observed when signal s_n^j is given. $p(s_n^j)$ is the *a priori* probability of the j^{th} signal being transmitted at interval *n*. This is usually a constant for each symbol being transmitted. The probability of receiving symbol R_n can be expressed as

$$p(R_n) = \sum_{j=0}^{M-1} p(R_n \mid s_n^j)\, p(s_n^j) \tag{14}$$

If $u_{n,i}$ is the i^{th} bit of the n^{th} received symbol then:

$$\begin{aligned} p(u_{n,i} = 0) &= \sum_{u_{n,i}=0} p(s_n^j \mid R_n) \\ &= \frac{\sum_{u_{n,i}=0} p(R_n \mid s_n^j)\, p(s_n^j)}{\sum_{j=0}^{M-1} p(R_n \mid s_n^j)\, p(s_n^j)} \end{aligned} \tag{15}$$

If the a priori probability $p(s_n^j)$ is the same for all symbols, (14) can be simplified as follows:

$$p(u_{n,i} = 0) = \sum_{u_{n,i}=0} p(R_n \mid s_n^j) \tag{16}$$

If σ_N ,is the variance of the noise, $p(R_n / s_n^j)$ in (15) can be expressed as

$$p(R_n \mid s_n^j) = \frac{1}{\sqrt{2ps_N}} \exp\left[-\frac{|R_n - s_n^j|^2}{2s_N^2} \right] \tag{17}$$

In the logarithmic domain the probability in (15) can be expressed approximately as

$$\begin{aligned} L(u_{n,i} = 0) &= \max_{u_{n,i}=0} [\ln(p(R_n \mid s_n^j))] \\ &= \max_{u_{n,i}=0} \left[-\frac{\left| R_{n-} s_n^j \right|^2}{2s_N^2} \right] \end{aligned} \tag{18}$$

where 'ln' is the natural logarithm. Then $L(u_{n,I}=0)$ can be found simply by taking the minimum value of the Euclidean distances calculated between the received signal and the signals of the 16QAM constellation where i^{th} bit equal to zero. Similarly $L(u_{n,I}=1)$ is also found. For the convolutional decoder (Soft input Viterbi) branch matrices are calculated as shown in the Table 2.

Table 2. Calculation of the branch metric for soft input Viterbi decoding

Bits at the branch (n)		Branch metric (n)
$n(1)$	$n(2)$	
0	0	$L(u_{n,I}=0) + L(u_{n,I}=0)$
0	1	$L(u_{n,I}=0) + L(u_{n,I}=1)$
1	0	$L(u_{n,I}=1) + L(u_{n,I}=0)$
1	1	$L(u_{n,I}=1) + L(u_{n,I}=1)$

For turbo decoder (max log MAP algorithm) the logarithm of likelihood ratio (LLR) associated with each bit has to be calculated. The LLR of the i^{th} bit in the n^{th} interval [25] can be expressed as

$$LLR(u_{n,i}) = K \log\left(\frac{p(u_{n,i}=0 \mid R_n)}{p(u_{n,i}=1 \mid R_n)}\right) \tag{19}$$

where K is a constant. Based on this, the result obtained in (17) and for K=1, we can find the LLR of the i^{th} bit as

$$LLR(u_{n,i}) = L(u_{n,i}=0) - L(u_{n,i}=1) \tag{20}$$

The transition probability corresponding to the transition from state σ_n to state σ_{n-1} can then be found using the LLR values obtained in (19).

$$g(s_n, s_{n-1}) = \text{LLR(systematic)} + \text{LLR(parity)} \tag{21}$$

- The investigated coding schemes possess characteristics such as high spectral efficient modulation and high coding gain required by broadband wireless communication systems.

- The concatenated schemes RS/TC and RS/T-TCM are capable of achieving good bit error rate performances in all the channels considered. Both concatenated schemes have about 2dB gain compared to other coding schemes. But the receiver complexities of these two codes are higher in terms of number of operations performed at the decoder. Therefore complexity of decoding has to be considered when these coding schemes are compared with each other.

E. Synchronization and sensitivity to frequency offset errors

There are two undesirable effects caused by frequency offset. First one is the reduction of signal amplitude in the output of the filters matched to each of the carriers. Second one is the introduction of inter channel interference (ICI) from the other carriers which are now no longer orthogonal. This is due to the fact, in OFDM the carriers are closely spaced in frequency compared with the channel bandwidth. Maintaining sufficient accuracy in frequency is difficult in mobile radio links, which also introduces significant Doppler shift [26].

The OFDM symbol representation with a frequency-offset y_k is given by (22). It consists of N complex sinusoids, which have been modulated with N complex modulation values X_n [26].

$$y_k = \frac{1}{N}\sum_{n=0}^{N-1} X_n H_n e^{j2pn(n+e)/N} + w_n \qquad (22)$$

where H_n is given in (6), ε is the relative frequency offset of the channel (the ratio of the actual frequency offset to the intercarrier spacing), and w_n is the complex envelope of the AWGN. It is assumed that the impulse response of the channel does not change during the symbol interval. The demodulation process, which is implemented with a FFT, consists of three components. The n^{th} element [26] at the demodulator output Y_n is given by

$$Y_n = (X_n H_n)\{(\sin pe)/N\sin(pe/N)\}.e^{jpe(N-1)/N} + I_n + W_n \qquad (23)$$

The first component is the modulation value X_n modified by the channel transfer function. This component experiences an amplitude reduction and phase shift due to the frequency offset. Since N is always much greater than pe , $N\sin(pe/N)$ can be replaced by . The second term I_n is the interchannel interference (ICI) caused by the frequency offset and is given by

$$I_n = \sum_{\substack{l=0 \\ l \neq n}}^{N-1} (X_l H_l)\{(\sin pe)/(N \sin(p(l-ne)/N))\}.e^{jpe(N-1)/N}.e^{-jp(l-n)/N}. \qquad (24)$$

The relationships for Y_n and I_n can be used to simulate the effect of frequency offset of the carrier on the average bit error rate.

V. Simulation Results

- Performances of the concatenated schemes were investigated in three different multipath channels. Power delay profiles of these theoretical channel models [9] can be expressed as

$$h_m = \begin{cases} (1+3.64\frac{m}{M})^{-3} & 0 \le m \le M \quad power\ 3\ decline \\ \exp(-4.6\frac{m}{M}) & 0 \le m \le M \quad \exp onential \\ 1 & 0 \le m \le M \quad uniform \end{cases}$$

where M is the total number of delayed paths. Corresponding channel models are depicted in Figure 9.

- The bit error rate performances of the coded OFDM systems in these multipath channels are depicted in Figure 10-Figure 12. For these results fading of the channels is considered to be independent. Figure 10 depicts the bit error rate performance of five concatenated coding schemes in a channel with a uniform power delay profile, having six delayed paths. It is clear that the lowest possible bit error rate is obtained using the T-TCM and TC concatenated

scheme. The performances of T-TCM and TC are obtained after six iterations, which increase the complexity of these schemes compared to the others (Table 3).

- T-TCM and TC schemes are capable of achieving a bit error rate less than 10^{-5} when the E_b/N_o is 6dB. They further achieves coding gain of about 1.5dB at bit error rate 10^{-5} compared to other coding schemes. Similar bit error rate performances were observed in other two channels as shown in Figure 11 and Figure 12.

- T-TCM and TC schemes have lower bit error rates compared to TCM1, TCM2 and CC schemes. We note that the bit error rate performance of TCM2 is better than that of TCM1. It is well known that the bit error rate performance becomes better when the number of states of a TCM scheme is increased [23]. This is true for TCM schemes used in OFDM systems also. Bit error rate performance of CC scheme is close to the performance of TCM2 scheme.

- CC scheme with 64 states is a popular coding scheme in wireless communications. The forward error correction codes used in IEEE 802.11 and HIPERLAN are based on this. As is seen, the bit error rate performance of both T-TCM and TC schemes are better than the performance of the industry standard CC code.

- 16QAM modulation is used with both TC and CC schemes so that the spectral efficiency is 2bits/s/Hz. This spectral efficiency is same as those used in other three coding schemes allowing a fair comparison of bit error rate performances. Next section presents the bit error rate performances observed in channels with correlated fading.

A. Bit error rate performance in a channel with correlated fading

- The simulation results given in Figure 13-Figure 15 were obtained under the assumption that the fading on the signal is correlated. In general mobile environment is frequency selective. In this case the correlation in phase and amplitude between two signals separated in frequency, is high for small frequency separation and falls essentially to zero as the separation substantially exceeds the correlation bandwidth.
- A channel interleaver is to be used in order to break the correlation of the signal. The

proposed channel interleaver is a 1024 8, symbol-block interleaver. The span and the depth of the interleaver is selected according to the following rules.

$$SP > \frac{KL}{R_{EN}}$$
$$LI \times SP > t(r)$$

Where *SP* and *LI* are the span and the depth of the interleaver, *KL* and R_{EN} are the constraint length of the trellis and the code rate of the encoder. $t(r)$ is the average fade duration.

- It is assumed that a fade occurs when the normalized signal power falls below -3dB. Then the average fade duration is 82μs, which is equal to 15 OFDM symbols. This resembles a slowly varying channel compared to the OFDM symbol duration. Therefore the channel can effectively be considered as static during an OFDM signal. For the TCM1 scheme the code rate of the encoder is 2/3 and the constraint length of the system is four. Therefore the span must be greater than six.

- Figure 13 depicts the bit error rate performances of coded OFDM schemes in a channel with uniform power delay profile and correlated fading. In this case also T-TCM and TC schemes perform better than other three schemes.

- It can be seen that both TC and T-TCM schemes have similar performances even in a fading channel. TC scheme has a coding gain greater than 2dB at bit error rate of 10^{-5} compared to TCM1, TCM2 and CC schemes. Both T-TCM and TC schemes are capable of achieving a bit error rate of 10^{-5} with an average E_b/N_0 of 8dB.

- This is a degradation of about 2dB compared to the bit error rate performance in a fully interleaved channel shown in Figure 10. Correlation of the fading in the channel degrades the bit error rate performance of the system.

- The use of interleaving reduces the degradation significantly. Although the channel interleaver used in our simulations is capable of achieving significant improvement, further improvement of the bit error rate performance is expected using a proper interleaving.

- Figure 14 and Figure 15 depict the performance of coding schemes in a correlated fading channels with exponential power delay profile and power three decline power delay profile respectively. There again both T-TCM and TC schemes show better bit error rate performances.

- Maximum frequency offset expected in the system is equal to the maximum possible Doppler shift (f_c=6.67 kHz). The relative frequency offset is then calculated with respect to the carrier separation. Carrier separation of the system considered is 183.5kHz. Therefore corresponding relative frequency offset is 0.036933.

- Figure 16 shows the bit error rate performance of the coding schemes in a channel with frequency offset. A channel with uniform power delay profile and a frequency offset is used for the simulation. As is seen, the degradation due to this frequency offset is negligible for all coding schemes considered.

- There is a 0.75dB degradation of the performance of T-TCM and 0.5dB degradation for TC scheme, while degradation in other schemes are much less. But with the increase in the frequency offset the performance degrades rapidly.

- For a frequency offset of $2f_c$ there is a degradation of 3 dB at a bit error rate of 10^{-4} for both T-TCM and TC schemes, while TCM scheme degrades by 2dB under that same conditions. It is interesting to note that the CC scheme does not degrade much compared to the other schemes, when the frequency offset increases. Degradation of CC scheme is only about 0.3dB at bit error rate of 10^{-4} for frequency offset of f_c and it is about 1dB when the frequency offset is $2f_c$.

- Figure 17 depicts the complementary cumulative density function (CCDF) of the PAPR (Pr(PAPR<PAPRo)) of a 512 carrier OFDM system. CCDF is the probability that the PAPR is less than a given threshold. It is clear that not all code-words of an OFDM signal result in a high PAPR. High peaks of the transmitted signal occur with very low probability [19]. From the figure it can be seen that the high peaks causing PAPR greater than 11.5dB occur with a probability less than 10^{-3}.

- Therefore clipping or windowing the high peak would not have considerable effect on bit error rate performance. But, If we deliberately clip the high peaks it will cause another undesirable effect, spectrum splatter. For this reason peak windowing is proposed in [19]. As it is already shown there, a window with good spectral properties has to be used. The window should be as narrowband as possible to reduce the effect of windowing on the other samples. We used a Hamming window of length 10 in our simulations. The corresponding windowing function is given by

$$1-\left(1-\frac{A}{X}\right)W(n) \qquad 0 \le n \le 10 \tag{25}$$

where $W(n)$, A and X are Hamming window, clip level and the amplitude of the corresponding peak respectively.

- Bit error rate performances of TCM1 scheme, obtained with different clip levels are shown in Figure 18. Curve 1 presents the bit error rate without peak windowing, while curves 2-5 present peak widowing at 6dB, 5dB, 3dB and 2dB respectively. As is seen, PAPR can be restricted to 6dB without noticeable degradation in bit error rate.

- When the peak windowing is used at 3dB degradation of more than 1dB is observed. Therefore it is clear that the peak windowing can be used to get the considerable peak power reduction without much degradation of the bit error rate performances. The complexity of using windowing to reduce PAPR is much less compared to the complexities of other schemes [16, 17]. Therefore, we suggest peak windowing for the proposed system. By using peak windowing complex PAPR reduction methods can be avoided.

VI. CONCLUSIONS

- The performances of orthogonal frequency division multiplexing with concatenated coding schemes are investigated in fading channels. ATM is used as the transport mechanism and a suitable mapping of ATM cells into OFDM symbols is proposed. A 512-carrier OFDM

system with a 10% guard interval, which is longer than the maximum delay spread of the channel is used.

- RS/T-TCM and RS/TC concatenated schemes have a high coding gain compared to other coding schemes and both schemes outperform TCM/RS scheme and RS/CC scheme in a frequency selective fading channels considered.

- When the complexity of the schemes are considered, TCM scheme has the lowest decoding complexity, while CC has a moderate complexity. But both T-TCM and TC schemes have higher complexities.

- If our objective is to find a suitable coding scheme with highest coding gain T-TCM would be our choice as it has lower complexity than TC although both have similar bit error rate performances. But, if we want to go for a scheme with a lowest complexity and having a reasonable bit-error-rate performance, TCM1 scheme would be our choice.

- Industry standard CC code with soft decision decoding falls in between above two categories, having a moderate decoding complexity and slightly better bit error rate performance compared to TCM. The performance degradation due to possible frequency offset due to Doppler effect is negligible in this system.

- But, it is observed that CC scheme has less sensitivity to frequency offset than other coding schemes. A relatively simple scheme of windowing the high peaks is used to limit the PAPR of the OFDM signal. PAPR can be reduced by about 5.5dB at 0.1% PAPR without noticeable bit error rate degradation. It can be concluded that investigated concatenated schemes will be potential candidates for the future broadband wireless networks. The performances of the proposed schemes are expected to improve with the use of a suitable ARQ scheme.

REFERENCES

[1] H. Nakamura, H. Tsuboya, M. Nakano, and M. Nakajima, "Applying ATM to mobile infrastructure networks," *IEEE Commun. Mag.*, vol. 36, no. 1, pp. 66-73, Jan. 1998.

[2] L. J. Cimini, "Analysis and Simulation of a Digital Mobile Channel Using Orthogonal Frequency Division Multiplexing," *IEEE Trans. Commun.*, vol. COM-33, no. 7, pp. 665-675, July 1985.

[3] M. Alard and R. Lassalle, "Principles of modulation and channel coding for digital broadcasting for mobile receivers,", EBU Technical review, no 224, 1987.

[4] B. L. Floch, R. Halbert-Lassalle, and D. Castelain, "Digital sound broadcasting to mobile receivers," *IEEE Trans. Consum. Elect.*, vol. 35, no. 3, pp. 493-503, Aug. 1989.

[5] J. S. Chow, J. C. Tu, and J. M. Coiffi, "A discrete multi-tone transceiver system for HDSL applications," *IEEE J. Select. Areas Commun.*, vol. 9, no. 6, pp. 895-908, Aug. 1991.

[6] S. Moriyama, K. Tsuchida, M. Sasaki, and S. Yamazaki, "Digital Outside-Broadcasting-Link Using OFDM Modulation Scheme," *IEEE Trans. Broad.*, vol. 42, no. 3, pp. 266-277, Sept. 1996.

[7] W. A. C. Fernando and R. M. A. P. Rajatheva, "Performance of turbo and trellis coded OFDM for LEO satellite channels in global mobile communications," in *Proc. IEEE ICC*, Atlanta, USA, pp. 56-60,1998.

[8] R. van-Nee and G. Awater, "New High-Rate Wireless LAN Standard," *IEEE Trans. Commun.*, vol. 37, no. 12, pp. 82-88, Dec. 1999.

[9] A. Chini, M. S. El-Tanany, and S. A. Mahmoud, "Transmission of High Rate ATM Packets over Indoor Radio channels," *IEEE J. Select. Areas. in Comm.*, vol. 14, no. 3, pp. 469-476, Apr. 1996.

[10] D. Dardari and V. Tralli, "High-Speed Indoor Wireless COFDM Systems at 60GHz: Performance and Design Criteria," in *Proc. IEEE GLOBECOM*, New York, NY, USA, pp. 1306-1311, 1997.

[11] H. Rohling and R. Gruneid, "Performance comparison of different multiple access schemes for the downlink of an OFDM communication system," in *Proc. VTC*, New York, NY, USA., pp. 1365-1369,1997.

[12] C. Berrou, A. Glavieux, and P. Thitimajshima, "Near Shannon limit error-correcting coding and decoding: Turbo-codes. 1," in *Proc. ICC*, Geneva., pp. 1064-1070, 1993.

[13] P. Robertson and T. Worz, "A novel bandwidth efficient coding scheme employing turbo codes," in *Proc. ICC*, pp. 962-967,1996.

[14] P. Robertson and T. Worz, "Bandwidth-Efficient Turbo Trellis-Coded Modulation Using Punctured Component Codes," *IEEE J. Select. Areas in Commun.*, vol. 16, no. 2, pp. 206-218, 1998.

[15] N. H. Ha and R. M. A. P. Rajatheva., "Performance of turbo trellis-coded modulation (T-TCM) on frequency-selective Rayleigh fading channels," *IEE Proc. Commun.*, vol. 146, no. 4, pp. 251-257, Aug. 1999.

[16] S. H. Muller and J. B. Huber, "A Comparision of Peak Power Reduction Schemes for OFDM," in *Proc. IEEE GLOBECOM '97*, New York, NY USA, pp. 1-5, 1997.

[17] J. A. Davis and J. Jedwab, "Peak-to-Mean Power Control in OFDM, Golay Complementary Sequences and Reed-Muller codes," *IEEE Trans. Commun.*, vol. 45, no. 7, pp. 2397-2417, Nov. 1999.

[18] D. Wulich and L. Goldfeld, "Reduction of peak factor in orthogonal multicarrier modulation by amplitude limitting and coding," *IEEE Trans. Commun.*, vol. 47, no. 1, pp. 18-21, Jan. 1999.

[19] R. van-Nee and A. D. Wild, "Reducing the Peak-to-Average Power Ratio of OFDM," in *Proc. IEEE VTC*, pp. 2072-2076, 1998.

[20] L. M. Correia and R. Prasad, "An Overview of Wireless Broadband Communications," *IEEE Commun. Mag.*, vol. 35, no. 1, pp. 28-33, Jan. 1997.

[21] J. G. Proakis, *Digital communications*, 3rd ed. New York: McGraw-Hill, 1995.

[22] A. Chini, Y. Wu, M. El-Tanany, and S. Mahmoud, "Filtered Decision Feedback Channel Estimation for OFDM Based DTV Terrestrial Broadcasting System," *IEEE Trans. Broad.*, vol. 44, no. 1, pp. 2-11, Mar. 1998.

[23] G. Ungerboeck, "Channel coding with multilevel/phase signals," *IEEE Trans.Info. Theory*, vol. IT-28, no. 1, pp. 55-67, Jan. 1982.

[24] S. B. Wicker, Error control systems for digital communications and storage: Prentice Hall, 1995.

[25] S. L. Goff, A. Glavieux, and C. Berrou, "Turbo-codes and high spectral efficiency modulation," in *Proc. ICC*, New Orleans, pp. 645-649,1996.

[26] P. Moose, "A Technique for Orthogonal Frequency Division Multiplexing Frequency Offset Correction," *IEEE Trans. Commun.*, vol. 42, no. 10, pp. 2908-2914, Oct. 1994.

[27] E. Biglieri, Introduction to trellis-coded modulation, with applications. New York: Macmillan, 1991.

[28] B. Vucetic, "Bandwidth efficient concatenated coding schemes for fading channels," *IEEE Trans. Commun.*, vol. 41, no. 1, pp. 50-61, Jan. 1993.

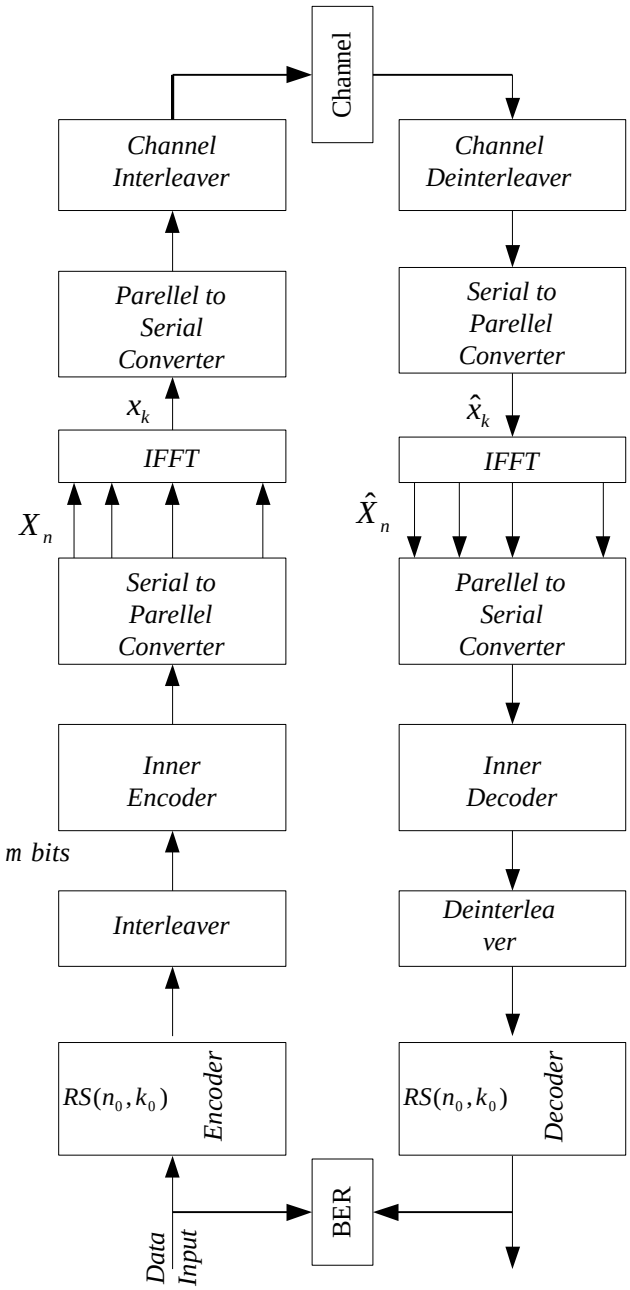

Figure 1 System model.

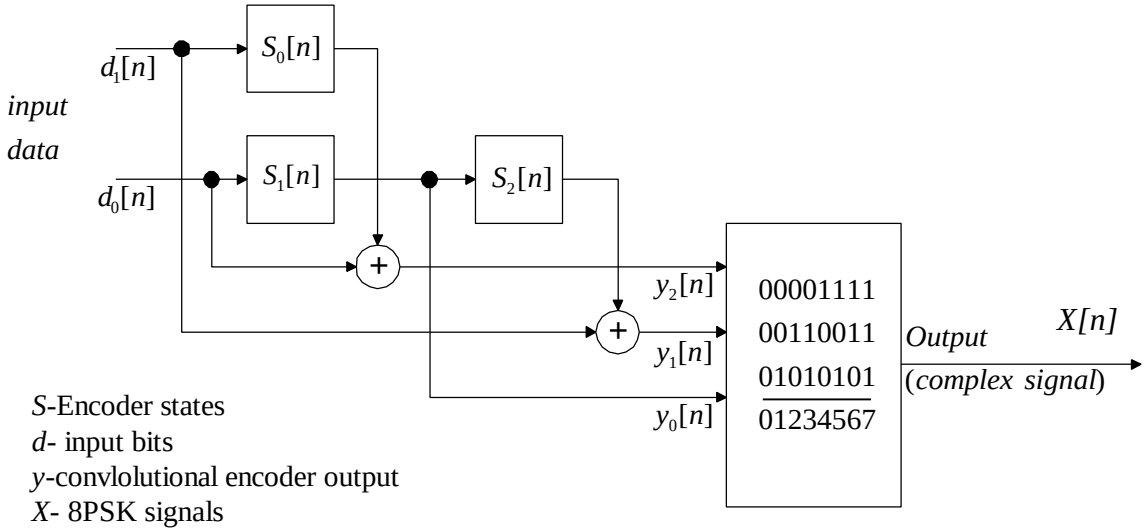

Figure 2. 8-state Ungerboeck encoder.

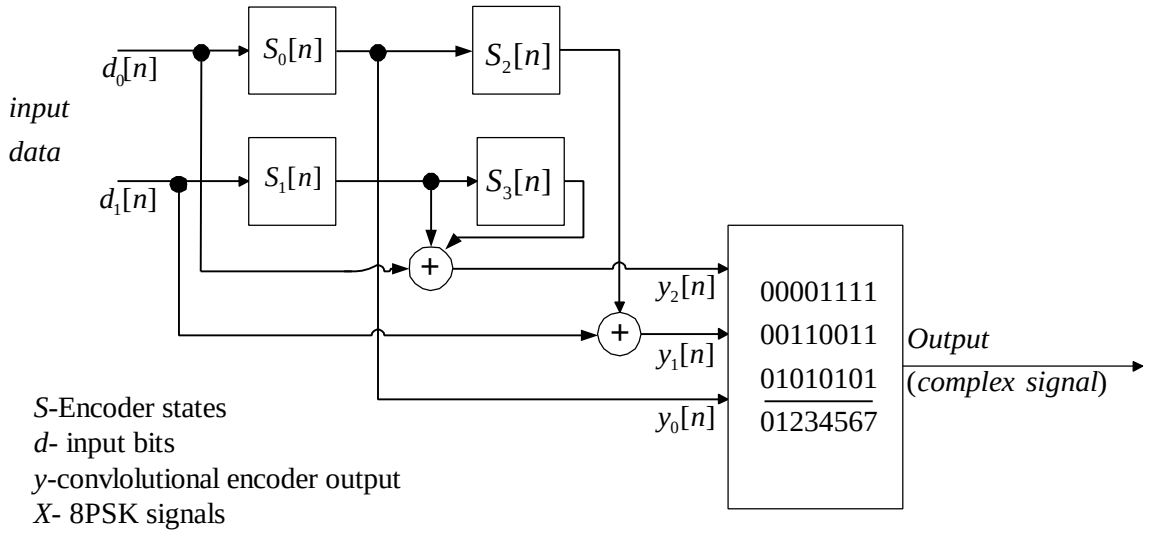

Figure 3. 16-state Ungerboeck encoder.

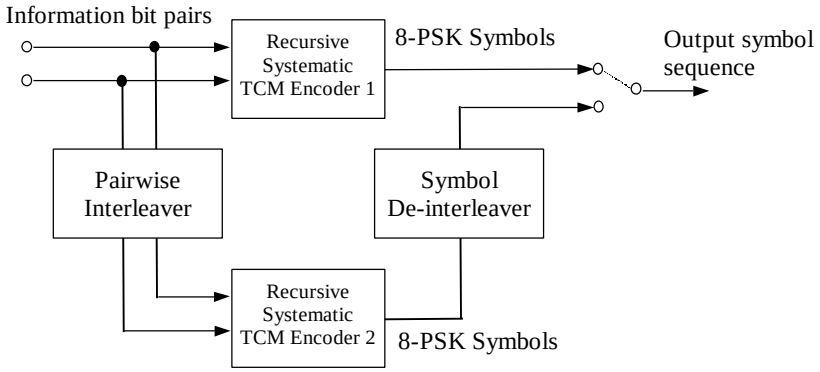

Figure 4 T-TCM encoder.

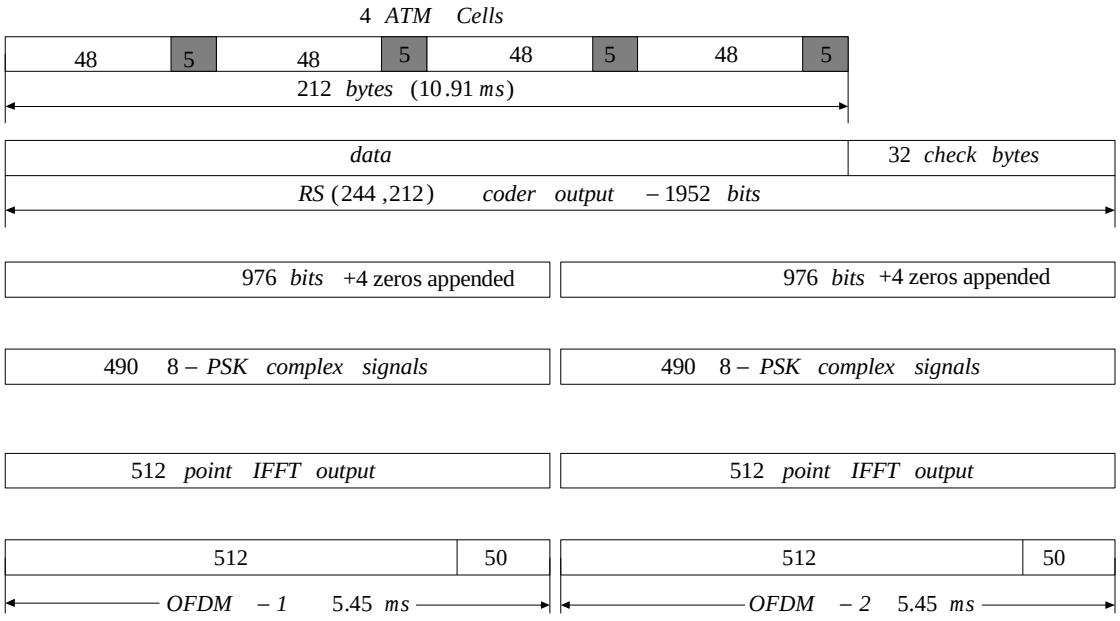

Figure 5 Mapping of ATM cells into OFDM symbols.

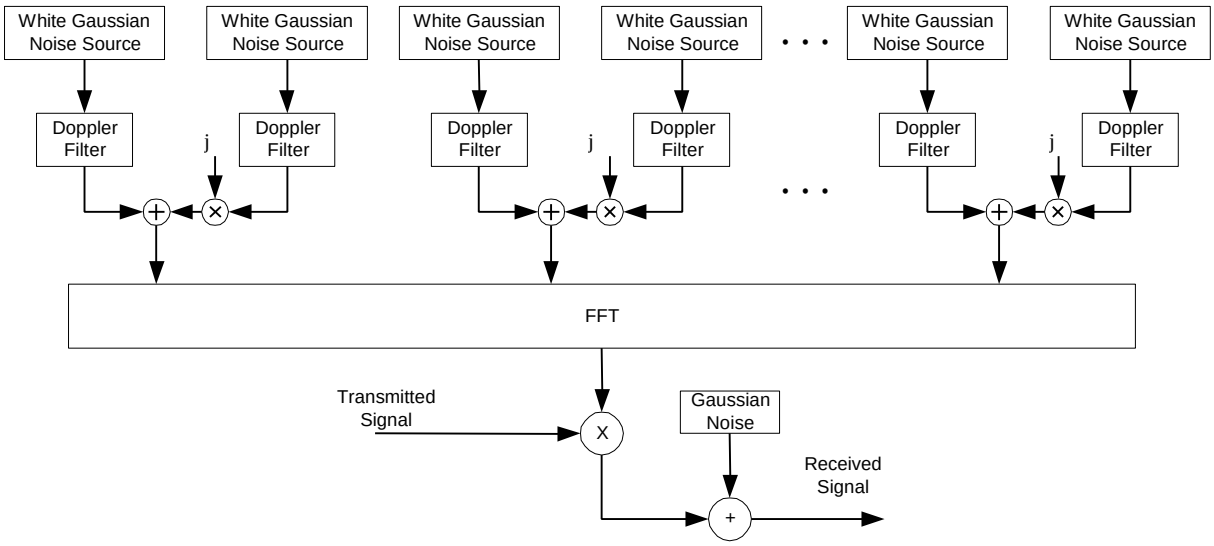

Figure 6 Frequency selective fading channel model for OFDM transmission.

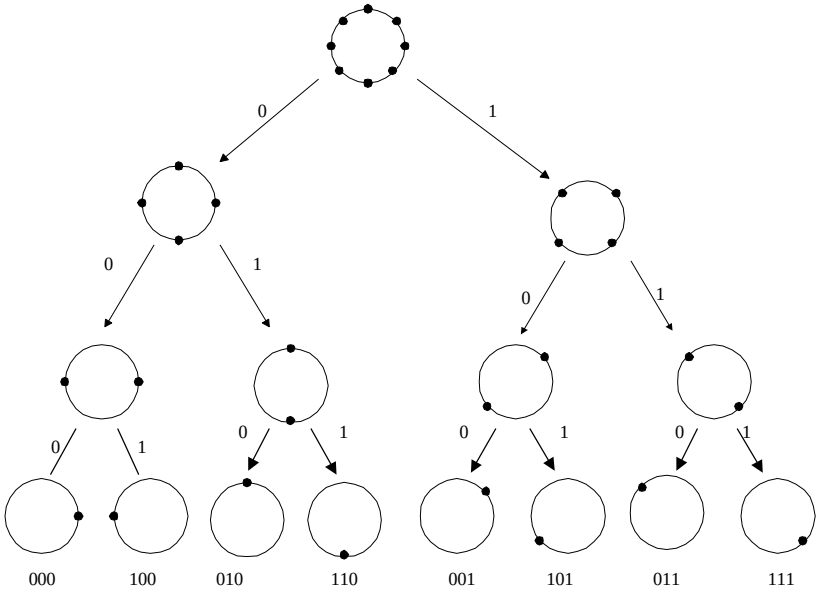

Figure 7 Set partition of the 8PSK constellation.

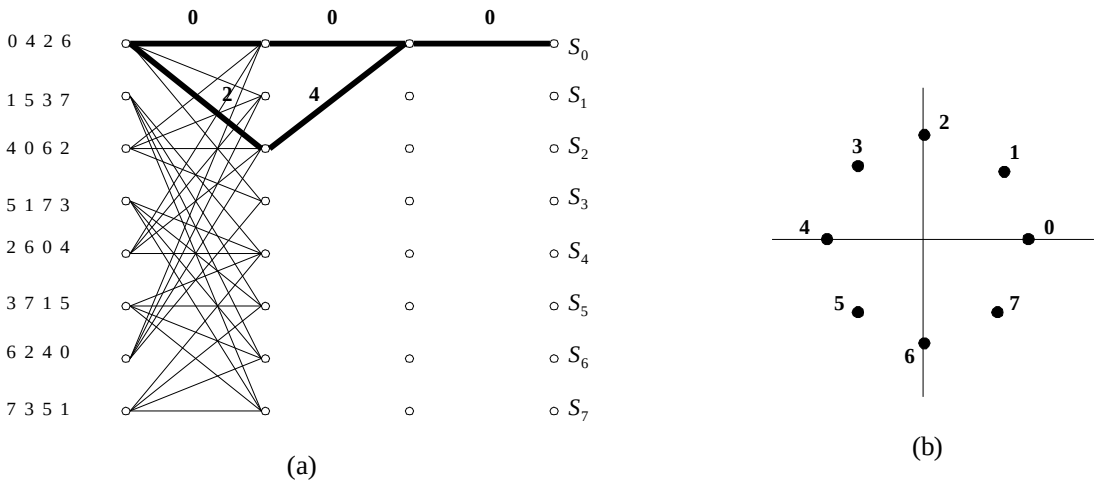

Figure 8 Rate 2/3 , 8 states Ungerboeck encoder using 8PSK mapping (a). Trellis diagram (b).signal constellation.

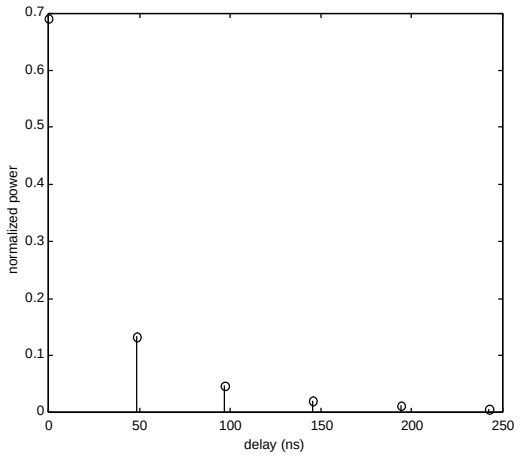

Power 3 decline power delay profile

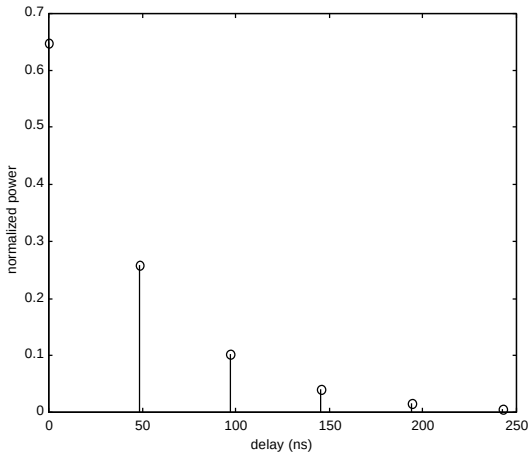

Exponential Power delay profile

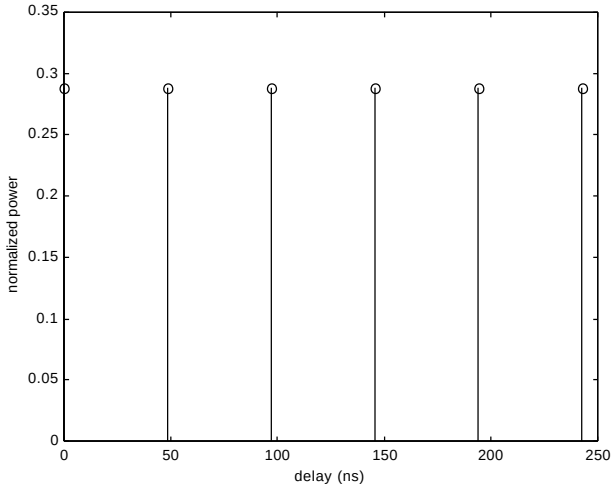

Uniform power delay profile

Figure 9 Channel Models.

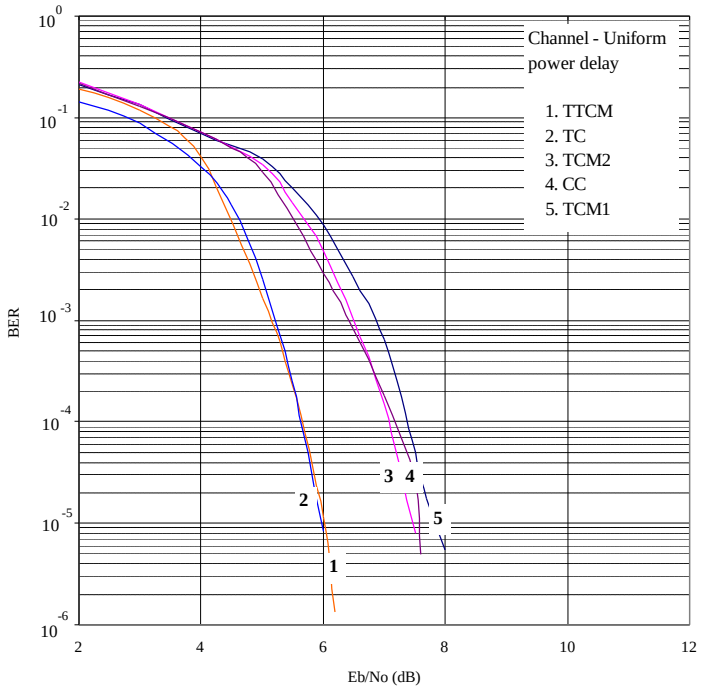

Figure 10 Comparison of performance of different coding schemes in a channel with uniform power delay profile and independent fading.

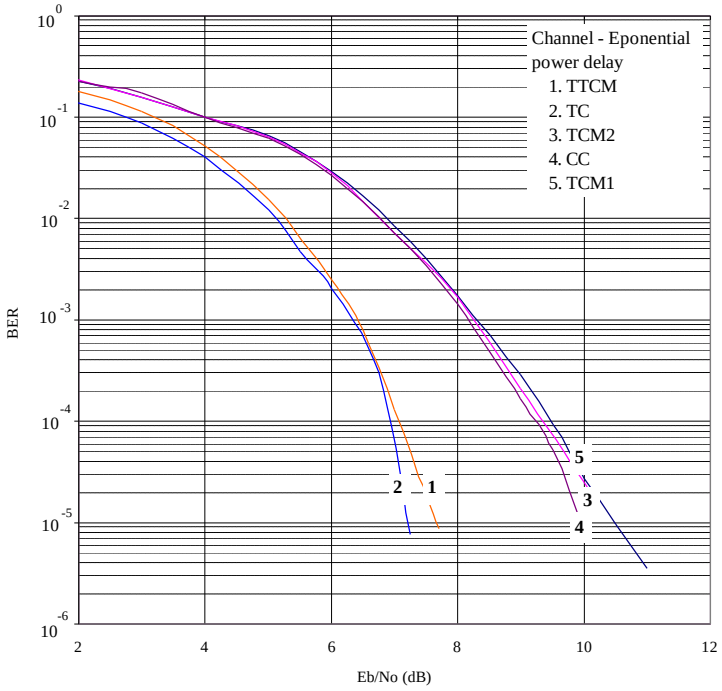

Figure 11 Comparison of performance of different coding schemes in a channel with exponential power delay profile and independent fading.

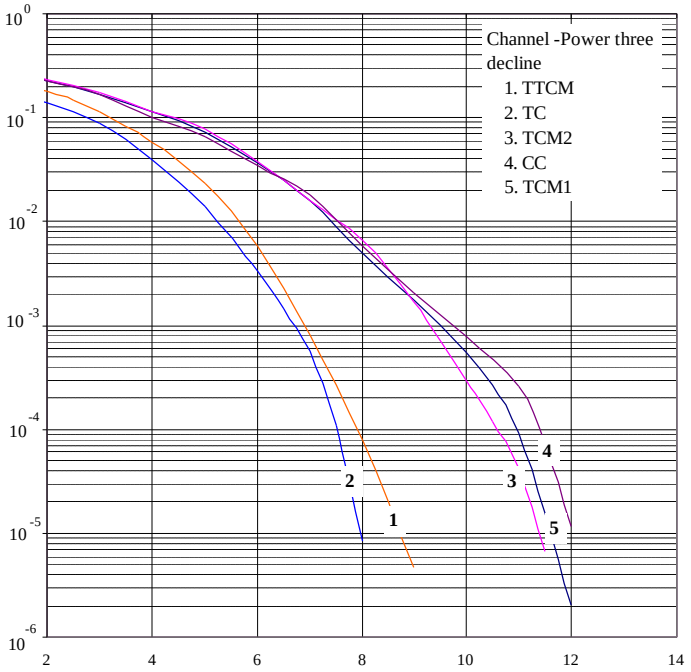

Figure 12 Comparison of performance of different coding schemes in a channel with power-three decline power delay profile and independent fading.

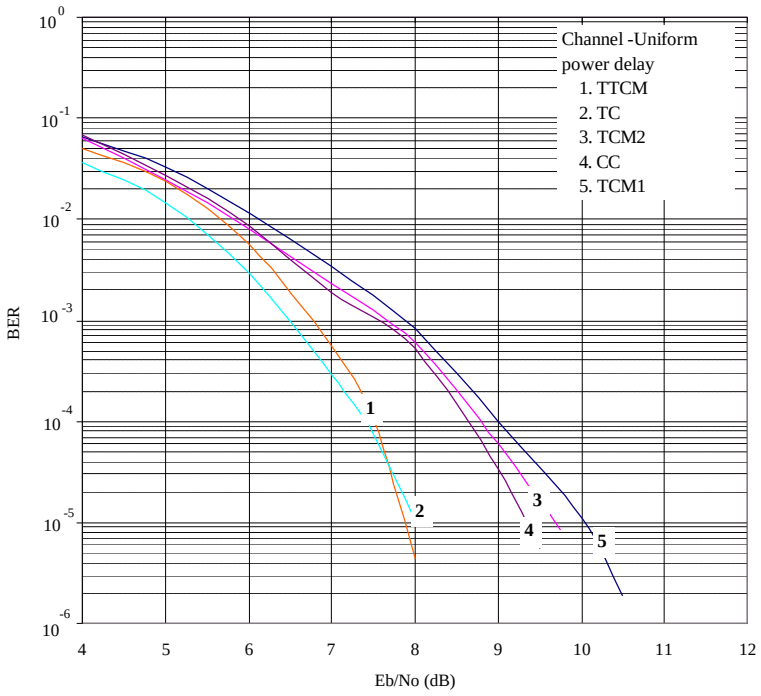

Figure 13 performance comparison of different concatenated coding schemes in a correlated fading channel with uniform power delay profile.

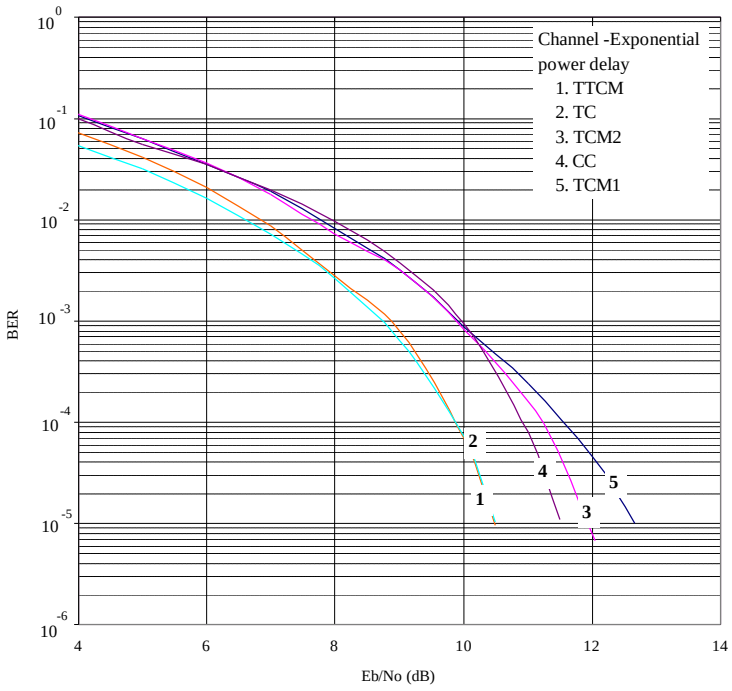

Figure 14 performance comparison of different concatenated coding schemes in a correlated fading channel with exponential power delay profile.

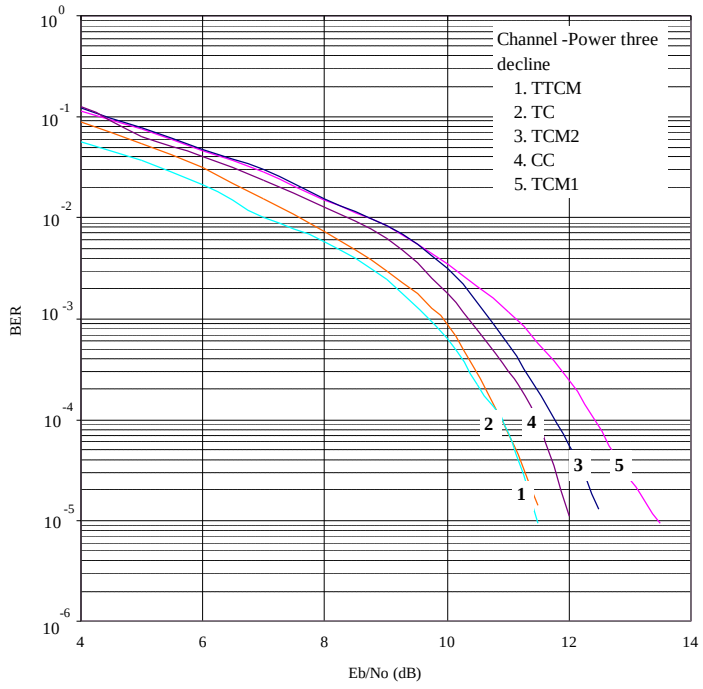

Figure 15 performance comparison of different concatenated coding schemes in a correlated fading channel with power three decline delay profile.

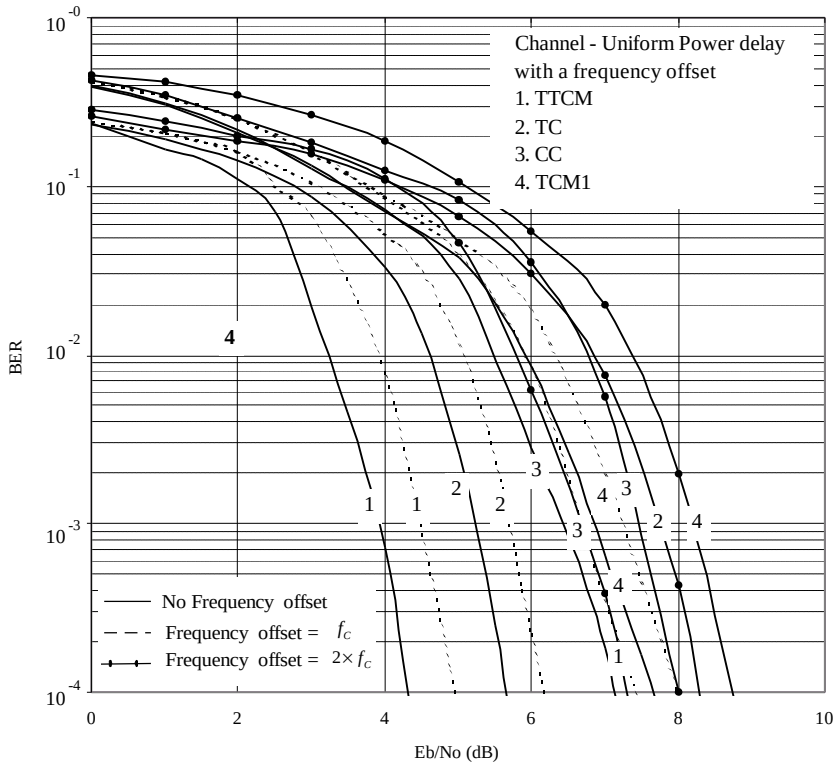

Figure 16 RS/TCM performance with frequency offset.

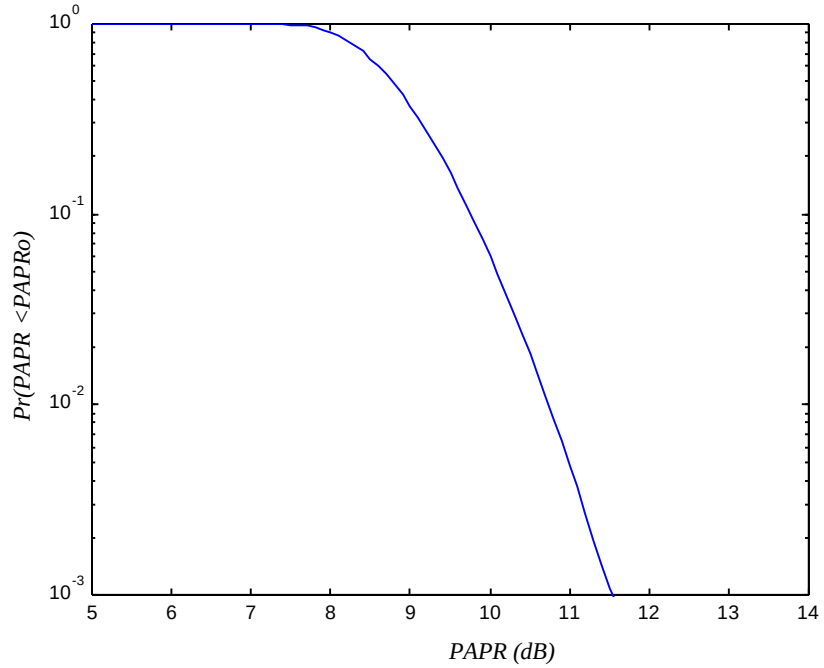

Figure 17 CCDF of an OFDM signal with 512 carriers.

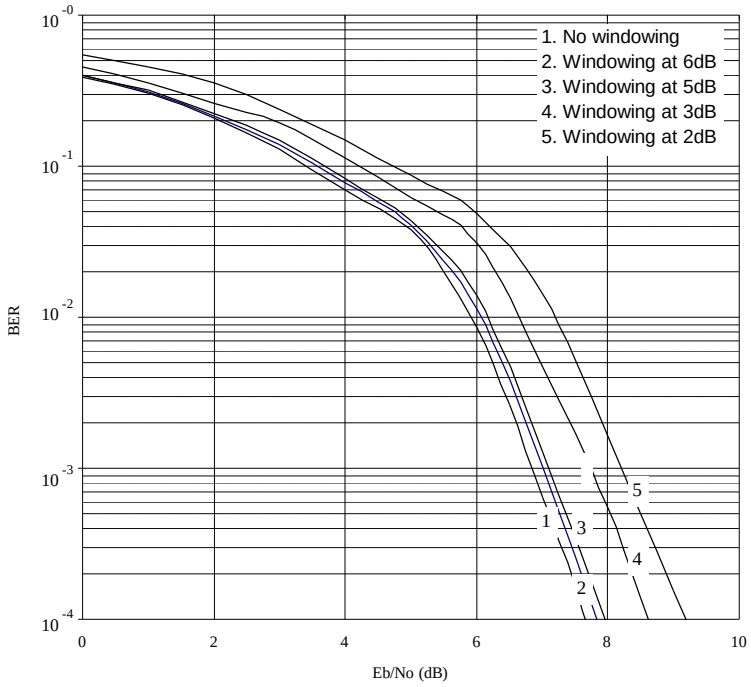

Figure 18 Bit error rate performance with peak windowing (TCM1).

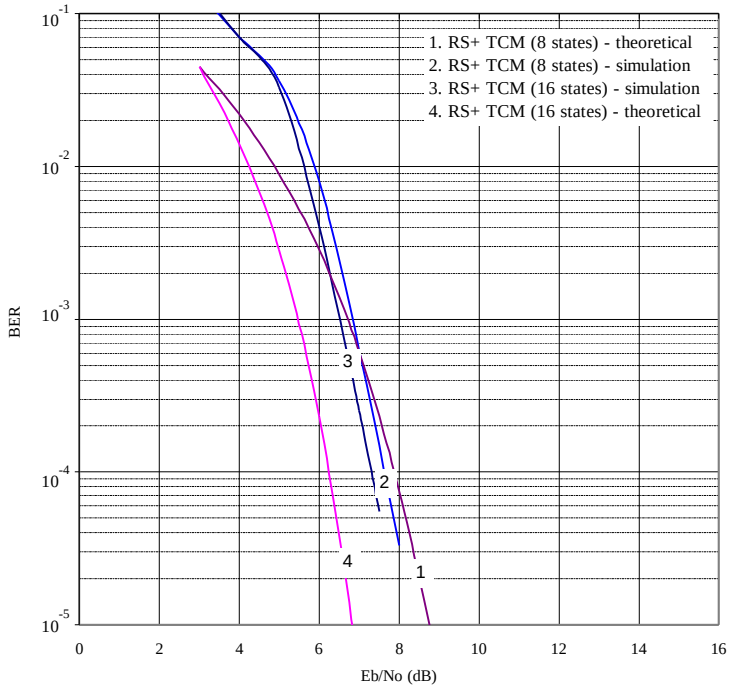

Figure 19 Theoretical upper bound and the simulation results for Ungerboeck's 8 state 8PSK code (TCM) in concatenation with RS(244,212) code.

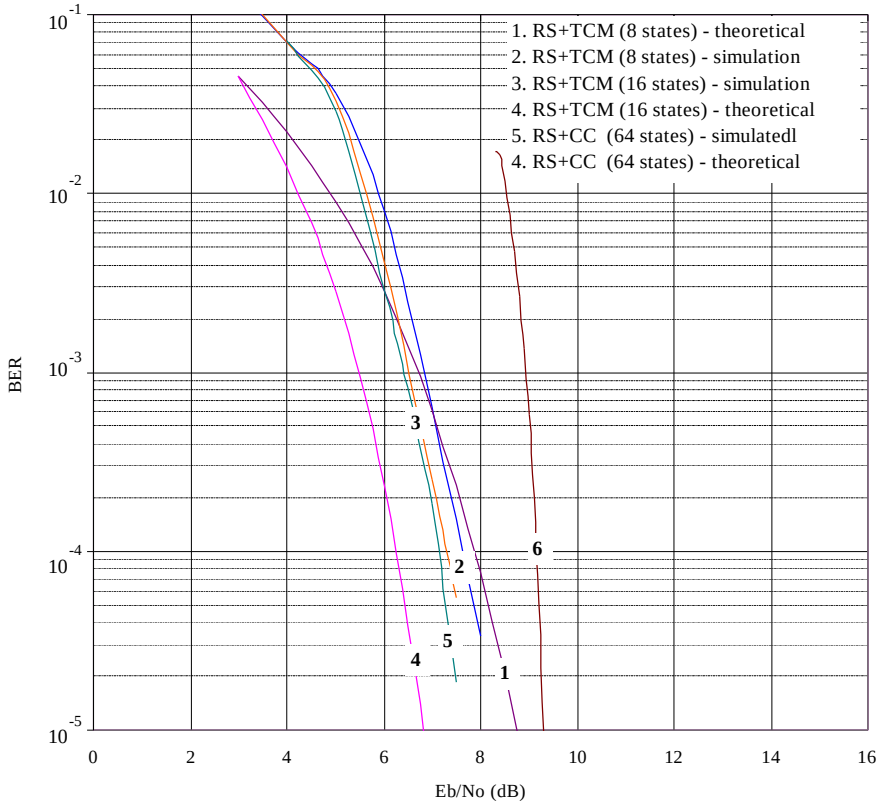

Figure 20 Comparison of theoretical and simulated results